ELSEVIER

Remote Sensing of Environment

Discrimination of Senescent Vegetation Using Thermal Emissivity Contrast

A. N. French, T. J. Schmugge,* and W. P. Kustas**

A remote sensing method utilizing multiband thermal infrared (8–12 μm) imagery that discriminates between senescent vegetation and bare soil is described. This discrimination is achieved by computing thermal band emissivities from a temperature-emissivity separation algorithm, and then classifying surface features based on spectral emissivity contrast. In a study of rangelands and winter wheat fields in central Oklahoma, the contrast, or range, of these spectral emissivities is diagnostic of the presence or absence of surface vegetative cover. A large range of emissivities, approximately greater than 0.03, is indicative of bare soil, while a low range, less than 0.02, is indicative of vegetative cover. When knowledge of the emissivity range is combined with a vegetation index, such as NDVI, the surface may be classified by a ternary system: bare soil, green vegetation, and senescent vegetation. Discrimination between bare soil and soil covered with senescent vegetation using emissivity contrast should be feasible in other settings. The benefit of this technique is that heat flux predictions can be based on a more accurate surface representation than otherwise provided by visible and near-infrared land classification schemes. Published by Elsevier Science Inc.

INTRODUCTION

The accurate parameterization of land surface characteristics is critical to reliably estimate surface heat fluxes from remote sensing platforms. In typical flux modeling schemes, characteristics such as vegetation canopy height, density, and albedo are related to surface roughness, fractional cover, and intercepted radiation. Since it is not feasible to determine in detail these characteristics directly, they are in turn estimated from land surface classifications obtained from a combination of ground observations and remote sensing data.

It is difficult, however, to create and maintain accurate land surface classification data sets, particularly over agricultural regions. While it may take weeks to develop and verify land use maps based on both ground observations and remote sensing data, the actual land use patterns and crop conditions will potentially change, perhaps several times, over a period of a few days. For example, a wheat crop could mature, be harvested, and the field plowed all after the time of classification.

One way to improve surface classification is to remotely collect diagnostic bands from the visible and near-infrared (VIS/NIR) bands simultaneously with brightness temperature data from thermal infrared bands. This will soon be feasible with a new sensor—ASTER (Advanced Spaceborne Thermal Emission and Reflection Radiometer; see http://asterweb.jpl.nasa.gov)—recently launched on the EOS-Terra satellite (Yamaguchi et al., 1998). ASTER simultaneously collects visible, near-infrared, and thermal-infrared data at spectral and spatial resolutions previously unavailable.

In our preparation for ASTER, we have been investigating the performance of heat flux models by combining remotely sensed Thermal Infrared Multispectral Scanner (TIMS; Palluconi and Meeks, 1985) data from aircraft and LANDSAT TM with ground observations. We have noticed that the land use images we develop using conventional VIS/NIR classification schemes fail to distinguish between senescent, or harvested vegetation, and bare plowed soil.

This inability has been noted elsewhere. Daughtry et al. (1995), for example, report that plant litter in general cannot be discriminated from bare soil based on any one particular visible or near-infrared reflectance. Under some circumstances litter can be discriminated by using three 50-nm bands over 2.0 to 2.2 microns (Nagler et al., 2000), but the technique is somewhat sensitive to moisture con-

* USDA/ARS Hydrology Laboratory

Address correspondence to A. N. French, Hydrology Lab, Building 007, BARC-WEST, USDA/ARS, Beltsville, MD 20705, USA. E-mail: anfrench@hydrolab.arsusda.gov

Received 15 November 1999; revised 10 March 2000.

REMOTE SENS. ENVIRON. 74:249–254 (2000)
Published by Elsevier Science Inc.
655 Avenue of the Americas, New York, NY 10010

0034-4257/00/$–see front matter
PII S0034-4257(00)00115-2

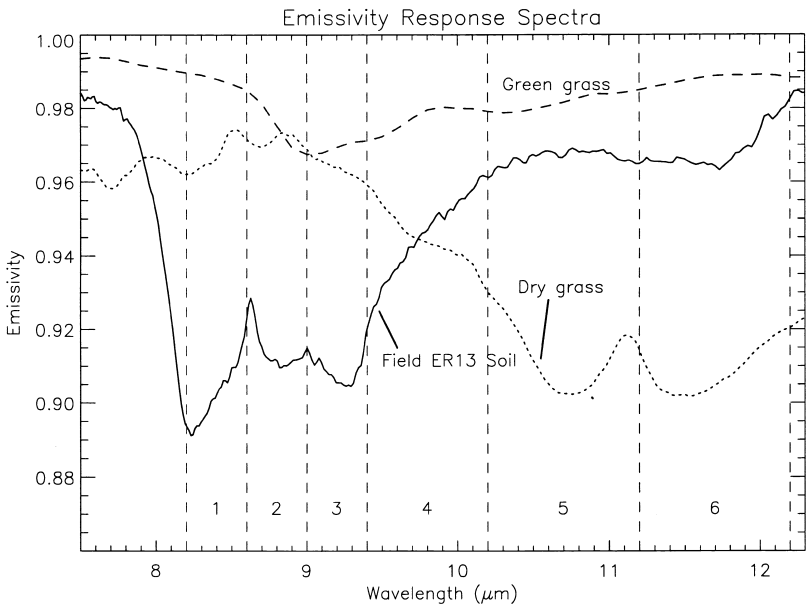

Figure 1. Emissivity response spectra for a quartz-bearing soil from field ER13, green grass sod, and dry grass sod (the last two from the ASTER spectral library). When remotely viewed, both green and dry grass are expected to have similar and nearly uniformly high emissivities ($\varepsilon \approx 0.98$). Dashed lines delineate TIMS bands.

tent and requires sensor bands unavailable on remote sensing platforms like ASTER.

Since the sensible and latent flux contributions from senesced vegetation and from bare soil are likely to be different, it is important to recognize the instances where there is ambiguity. But rather than just account for the ambiguity, we have found that the ambiguity can be removed if thermal-infrared data is included in the land surface discrimination scheme.

THE THERMAL EMISSIVITY CONTRAST METHOD

The scheme proposed here is to combine the well-known VIS/NIR vegetation index, NDVI, with a thermal-band emissivity contrast image. Thermal emissivity contrast is simply the range of observed emissivities for a given image pixel. It is mainly a function of material properties, such as vegetative cover and soil mineralogy, and is insensitive to surface temperature variations.

Emissivity, a dimensionless quantity ε, represents the ratio of a material's spectral radiance, L, to a perfect blackbody spectral radiance, L_{BB}, at a given temperature [see Eq. (1)]:

$$\varepsilon = \frac{L}{L_{BB}} \tag{1}$$

Emissivities of surface materials vary with wavelength. The variation may be strong, as for bare soil, or weak, as for green grass (Fig. 1). If emissivity of a material is sampled in the same manner as for VIS/NIR sensors by using several bands, its approximate emissivity signature can be determined. For example, note that the abrupt jump in emissivity for bare soil from El Reno field ER13 at $\approx 9.5\ \mu$m in Fig. 1 is also abrupt when TIMS bands 3 and 4 are compared (Table 1).

Emissivity spectra are distinctive for many common soils because they usually contain two quartz restrahlen bands between 8 and 9 μm. Since most soils contain quartz minerals, the emissivity profile may have a wide range, or contrast, from about $\varepsilon = 0.80$ at 9 μm up to $\varepsilon = 0.98$ at 12 μm (Salisbury and D'Aria, 1992a). Emissivity spectra may not be diagnostic, however, if the soil texture is very fine or if the surface moisture content is significant (Salisbury and D'Aria, 1992b).

Plant matter spectra (Elvidge, 1988), on the other hand, are distinct from soil spectra. Both green and senescent vegetation have high emissivities with a small range when viewed as a plant canopy (Palluconi et al., 1990). Alternatively, vegetation may have high emissivities in the 8-μm to 9-μm wavelengths and low emissivities in the 9.5-μm to 12-μm wavelengths (Table 1) when viewed as individual leaves. In remote sensing applications, this drop in emissivity with increasing wavelengths probably would not be observable because vegetation is usually resolved as a canopy. Despite this potential ambiguity, plants can be distinguished from bare soils because their emissivity spectra can differ by $\Delta\varepsilon \geq 0.06$. When plant emissivities are combined with NDVI measurements that identify green vegetation, the land surface may be remotely identified as bare soil, green vegetation, or senescent vegetation.

The best way to obtain thermal band emissivities is a subject of current research, and a range of approaches are used. Reviews of many of them may be found in Li et al. (1999), as well as in Hook et al. (1992). The particular technique used for this study is based on the temperature-emissivity separation (TES) algorithm, which may resolve surface temperatures within 1.5 K and $\Delta\varepsilon \leq 0.015$ (Gillespie et al., 1998; Schmugge et al., 1998). In brief, the TES

Table 1. TIMS Band-Averaged Emissivities

	TIMS Bands					
Material	*1*	*2*	*3*	*4*	*5*	*6*
ER13 soil	0.908	0.912	0.910	0.953	0.967	0.967
Green grass	0.987	0.973	0.970	0.979	0.982	0.988
Dry grass	0.969	0.971	0.962	0.939	0.910	0.908

Field ER13 emissivities are from soil measurements by Cindy Grove. The green grass and the dry grass measurements are from "large piece[s] of sod," as described in the ASTER spectral library (Salisbury and D'Aria, 1992a). At this scale, green grass is spectrally distinct from dry grass, but would not be when viewed remotely. Comparably detailed spectra of vegetation canopies are, to our knowledge, unavailable.

method makes use of an empirical relation between the range of emissivities and the minimum emissivity. TES is sensitive to uncertainties in atmospheric water vapor (Coll et al., 1998), as well as to instrument calibration. Consequently, these effects need to be removed if reliable surface temperatures and emissivities are to be obtained. Provided these adjustments are made, observed brightness temperatures from the different thermal bands will be nearly equal when observing a surface with no emissivity contrast; in other words, when the surface is a blackbody or a graybody. When the brightness temperatures from the thermal bands differ greatly, as in the ER13 soil sample mentioned earlier, the surface is not a blackbody or graybody because its emissivity is wavelength dependent.

In TES, relative emissivities, β_i, are derived for each band, where ε_i represents band emissivities using Eq. (1) and represents the average emissivity over all bands [see Eq. (2)]:

$$\beta_i \equiv \frac{\varepsilon_i}{\bar{\varepsilon}} \tag{2}$$

The maximum range of values, denoted as *MMD* (Maximum-Minimum apparent emissivity Difference), is then used to compute the minimum emissivity, $\varepsilon_{\min}$ [see Eq. (3)]:

$$\varepsilon_{\min} = a - b * MMD^c \tag{3}$$

where a, b, and c are constants determined from experimental data. The remaining band emissivities can then be solved with Eq. (4):

$$\varepsilon_i = \varepsilon^{\min} * \left[\frac{\beta_i}{\min(\beta_i)} \right]. \tag{4}$$

RESULTS

Land classification using thermal emissivity contrast can be demonstrated using remotely sensed data collected on 2 July 1997 during the Southern Great Plains 1997 experiment (SGP97) in Oklahoma, USA (see http://hydrolab.arsusda.gov/sgp97/ for details). Thermal infrared data collected over the study site at El Reno were combined with visible near-infrared data to perform the analysis. The thermal infrared data were collected from an aircraft using the 12-band TMS (Thematic Mapper Simulator) Daedalus 1268 scanner. Nearby balloon sondes were used to determine an atmospheric profile, and the MODTRAN program (Berk et al., 1998) was used to generate average atmospheric transmissivity and radiance for each of the thermal bands. When the TES algorithm was applied, a histogram of the resulting emissivity contrast image revealed a bimodal distribution (Fig. 2) and was representative of the relative abundance of vegetated and bare surfaces. Most of the scene had low emissivity contrast, $\Delta\varepsilon \leqslant 0.036$, except for the bare soils, which had contrasts of $0.04 \leqslant \Delta\varepsilon \leqslant 0.07$. An image of the emissivity contrast is shown in Fig. 3A, where dark tones indicate low contrast and light tones indicate contrast of 0.03 or greater. The computed NDVI for the same area (Fig. 3B) indicates low abundance of green vegetation by dark tones and abundant green vegetation, with Leaf Area Indices (LAI) greater than 2 indicated by light tones.

When emissivity contrast data is jointly plotted with NDVI data, three landscape types can be classified as follows (Fig. 4):

1. Green vegetation, as in field ER09, had relatively high NDVI (≈ 0.37) and low emissivity contrast ($\Delta\varepsilon \approx 0.016$).
2. Bare soil, as in field ER13, had low NDVI (≈ -0.1) and high emissivity contrast ($\Delta\varepsilon \approx 0.055$).
3. Senescent vegetation, as in the harvested (but untilled) winter wheat field ER10, had low NDVI (≈ -0.1) and low emissivity contrast ($\Delta\varepsilon \approx 0.015$).

Ground observations of the El Reno fields confirm these relationships and are listed in Table 2. Field ER09 had a high average LAI of 2.7, 78% of which was green vegetation (green LAI of 2.14). Field ER10 had a low LAI of 0.65, none of which was green. Wet biomass of ER10, consisting of harvested wheat stubble and residue, is close to double that of ER09. Field ER13, because it had been recently plowed, had no significant vegetation.

DISCUSSION

The emissivity contrast image over El Reno fields shows that bare soils had a relatively high thermal emissivity range

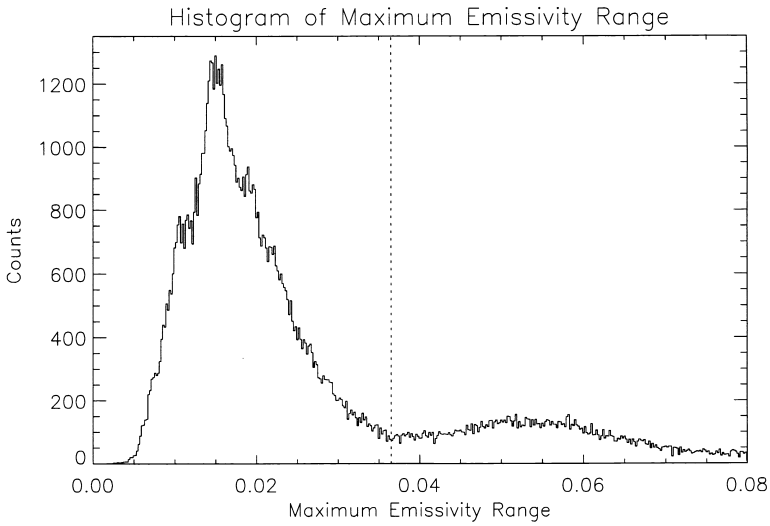

Figure 2. Histogram of subset of El Reno flight line 1, run 3, on 2 July 1997 (image shown in Fig 3A). Most of the scene had emissivity variations less than ≈0.36, corresponding to vegetated or residue-covered surfaces. Bare soil surfaces, to the right of the dashed line, had emissivity variations of 0.04 to over 0.07. The discrete nature of the El Reno fields causes the bimodal distribution of emissivity contrast and simplifies categorization of vegetative cover vs. bare soil. Other sites with a more uniform distribution of fractional vegetative cover would require ground observations to determine the minimum emissivity contrast that best represents bare soil.

($\Delta\varepsilon \approx 0.05$), but that covered soils had a low range ($\Delta\varepsilon < 0.02$). This distinction is supported by uncertainty estimates. Based on spatial variations within fields ER10 and ER13, emissivity contrast uncertainty was $\Delta\varepsilon \approx \pm 0.01$, significantly less than the mean emissivity separation of $\Delta\varepsilon \approx 0.04$. The ability to discriminate bare soils from covered soils can be combined with NDVI's ability to discriminate green vegetation from the absence of green vegetation to yield three land classifications: bare soil, soil covered with green vegetation, and soil covered with nongreen vegetation. Bare soils are distinguished by high emissivity contrast and low NDVI. Soils covered by green vegetation have low emissivity contrast and high NDVI. Soils covered by nongreen, or senescent, vegetation have low emissivity contrast and low NDVI.

Because the land surfaces at El Reno consisted of nearly homogeneous and discrete grasslands, wheat fields, and bare soil fields, the relationship between emissivity contrast and vegetated cover were easily observed. The histogram of emissivity contrast for the El Reno area (Fig. 2) naturally separated bare soil surfaces from surfaces covered by green and senescent vegetation at $\Delta\varepsilon \approx 0.036$. But

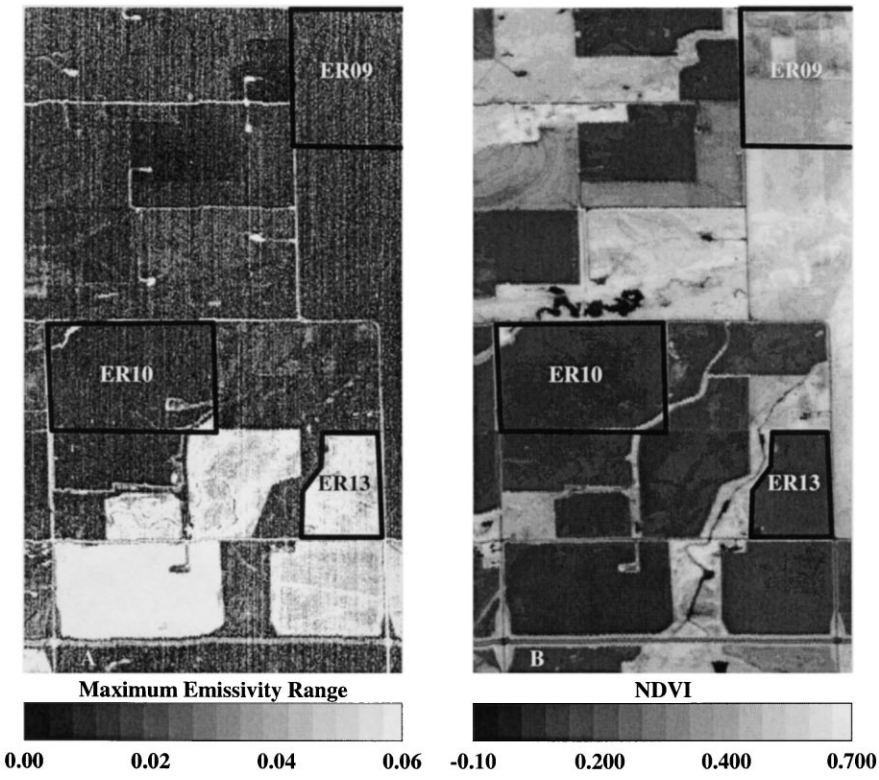

Figure 3. Images of El Reno fields, 2 July 1997 (aircraft altitude 5 km above ground level, pixel size 12 m). Three different land surfaces in the El Reno study area are outlined: a pasture (ER09), a harvested winter wheat field (ER10), and a plowed winter wheat field (ER13). Each image covers approximately 5 km north to south (north is toward the top) and 2 km east to west. Maximum range emissivity, shown at the left (A), is scaled for contrasts between 0.00 to 0.06. NDVI, shown at the right (B), ranges from −0.1 to +0.7. Fields ER10 and ER13 are indistinguishable in the NDVI scene, but are easily distinguished in the emissivity scene.

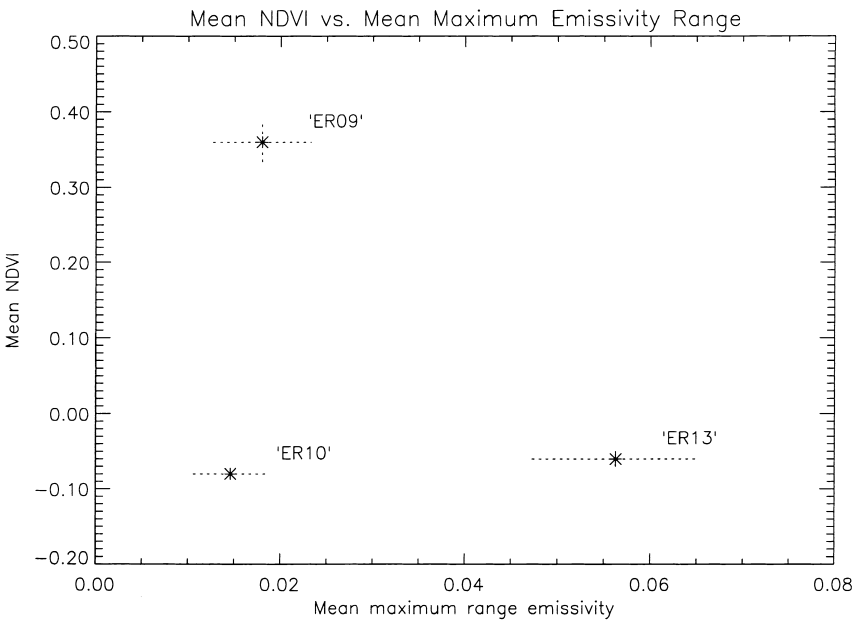

Figure 4. Cross-plot of mean NDVI vs. mean maximum range of emissivity, based on the scene shown in Fig. 3. Asterisks indicated mean NDVI and mean maximum emissivities for each field. Standard deviations, indicated by dashed lines, show that there is greater variability in emissivity contrast than in NDVI, but that the plowed field (ER13) is nevertheless distinct from the harvested winter wheat field (ER10). Nearly identical results were obtained from a 1.5-km altitude flight on the same day and similar time.

this separation cannot be expected to be distinctive in general, particularly where the landscape consists of a more uniformly distributed range of vegetative cover. In these cases, local observations of surface conditions would be required to help determine the relationship between vegetated cover and emissivity contrast. With such observations it might be possible to not only categorize the surface as covered or bare, but also to infer fractional vegetation cover from emissivity contrast. Current results at El Reno, however, are insufficient to support this additional capability.

Distinguishing between the three cover conditions (green vegetation, senescent vegetation, and bare soil) is important because the cover strongly influences the surface thermal gradient, surface roughness, and the consequent surface heat flux. For example, sensible heat flux (H) from a bare soil surface may be parameterized as a single source, but if the surface is covered, there are two sources of heat flux: vegetation and soil. Dead vegetation increases surface roughness, acting as a canopy with no latent heat flux (LE). It also reduces the amount of radiant energy at the soil surface.

These effects can be demonstrated over wheat stubble in field ER10. Using TES-computed temperatures along with a parallel two-source model described and tested in French et al. (2000), heat fluxes were predicted in two ways: first by modeling field ER10 as a bare soil surface, and second by modeling the field as a canopy of senescent vegetation. As shown in Table 3, the inclusion of dead vegetation canopy potentially can reduce the soil sensible heat flux (H from soil) and ground heat flux (G). G is lower because less radiation reaches the soil surface (Kustas and Norman, 1999). H from soil is lower with a canopy layer because resistance to heat transport is larger. The total predicted H for either surface condition, however, remains essentially the same. Soil latent heat flux (LE from soil) is higher for the wheat stubble surface, possibly because the soil remained relatively wetter when shielded by vegetation.

CONCLUSIONS

Remote sensing data from the SGP97 El Reno study show that senescent vegetation can be distinguished from bare soil surfaces using thermal infrared emissivity differences. When combined with VNIR, the thermal emissivity contrast technique can improve results from heat flux models through better land surface classification. Thermal emissivity contrast may be especially useful for energy balance modeling in agricultural areas where distinguishing be-

Table 2. El Reno Fields: Ground Observations

Field	*Land Use*	*Total LAI*	*Green LAI*	*Wet Biomass (g m^{-2})*
ER09	Pasture	2.73	2.14	368.7 (23.7)
ER10	Wheat (harvested)	0.65	0.00	675.3 (36.1)
ER13	Bare soil	0.00	0.00	0.00

The leaf area indices and wet biomass entries are averages of three samples within a field. Standard deviations for wet biomass are indicated in parentheses.

Table 3. El Reno Field ER10, Modeled as Bare Soil and as Wheat Stubble

Surface	*H from Soil*	*H from Canopy*	*LE from Soil*	*LE from Canopy*	*G*	*Rn*
Bare soil	254 (90)	0 (0)	103 (91)	0 (0)	153 (2)	510 (7)
Wheat stubble	115 (9)	127 (3)	157 (18)	0 (0)	116 (3)	515 (6)

Listed are model-predicted sensible heat fluxes (H), latent heat fluxes (LE), ground heat fluxes (G), and net radiation (Rn) values, all in Wm^{-2}. Mean surface temperature was 45°C and mean NDVI was −0.08. Standard deviation of fluxes within the field are indicated in parentheses.

tween bare soils and harvested fields can lead to significant changes in energy partitioning.

Extension of the method to other areas will require an approach similar to the one used at El Reno. Multiband thermal infrared data, good estimates of atmospheric water vapor, a few confirmatory ground observations of field conditions, and emissivity spectra of typical soils would all be required. Future research may show that it is feasible to estimate degree of fractional vegetative cover from emissivity contrast.

The ASTER project provided support for the aircraft flights and resources for the data analysis. Cindy Grove, Jet Propulsion Laboratory, Pasadena, California made the soil emissivity measurements. Vegetation data were provided by C. S. T. Daughtry of the USDA-ARS Remote Sensing and Modeling Lab.

REFERENCES

Berk, A., Bernstein, L., Anderson, G., Acharya, P., Robertson, D., Chetwynd, J., and Adler-Golden, S. (1998), MODTRAN cloud and multiple scattering upgrade with application to AVIRIS. *Remote Sens. Environ.* 65:367–375.

Coll, C., Schmugge, T. J., and Hook, S. J. (1998), Atmospheric effects on the temperature emissivity separation algorithm. In *EUROPTO Conference on Remote Sensing for Agriculture, Ecosystems, and Hydrology, SPIE*, vol. 3499, pp. 405–415.

Daughtry, C., McMurtrey, J., Chappelle, E., Dulaney, W., Irons, J., and Satterwhite, M. (1995), Potential for discriminating crop residues from soil by reflectance and fluorescence. *Agron. J.* 87:165–171.

Elvidge, C. D. (1988), Thermal infrared reflectance of dry plant materials: 2.5–20.0 μm. *Remote Sens. Environ.* 26:265–285.

French, A., Schmugge, T., and Kustas, W. (2000), Estimating surface fluxes over the SGP site with remotely sensed data. *Phys. Chem. Earth (B)* 25(2):167–172.

Gillespie, A., Rokugawa, S., Matsunaga, T., Cothern, J., Hook, S., and Kahle, A. (1998), A temperature and emissivity separation algorithm for Advanced Spaceborne Thermal Emission and Reflection Radiometer (ASTER) images. *IEEE Trans. on Geo. Remote Sens.* 36:1113–1126.

Hook, S. J., Gabell, A., Green, A., and Kealy, P. (1992), A comparison of techniques for extracting emissivity information from thermal infrared data for geological studies. *Remote Sens. Environ.* 42:123–135.

Kustas, W., and Norman, J. (1999), Evaluation of soil and vegetation heat flux predictions using a simple two-source model with radiometric temperatures for partial canopy cover. *Agric. For. Meteorol.* 94:13–29.

Li, Z.-L., Becker, F., Stoll, M. P., Wan, Z. (1999), Evaluation of six methods for extracting relative emissivity spectra from thermal infrared images. *Remote Sens. Environ.* 69:197–214.

Nagler, P., Daughtry, C., and Goward, S. (2000), Plant litter and soil reflectance. *Remote Sens. Environ.* 71:207–215.

Palluconi, F., Kahle, A. B., Hoover, G., and Conel, J. E. (1990), The spectral emissivity of prairie and pasture grasses at Konza Prairie, Kansas. In *Proc. of the Amer. Meteorol. Soc. Symposium on the First ISLSCP Field Experiment (FIFE),* American Meteorological Society, pp. 77–78.

Palluconi, F. D., and Meeks, G. R. (1985), Thermal Infrared Multispectral Scanner (TIMS): An investigator's guide to TIMS data, *Tech. Rep. JPL Publication 85–32,* Jet Propulsion Laboratory, California Institute of Technology, Pasadena, CA.

Salisbury, J. W., and D'Aria, D. M. (1992a), Emissivity of terrestrial materials in the 8–14 μm atmospheric window. *Remote Sens. Environ.* 42:83–106.

Salisbury, J. W., and D'Aria, D. M. (1992b), Infrared (8–14 μm) remote sensing of soil particle size. *Remote Sens. Environ.* 42:157–165.

Schmugge, T., Hook, S., and Coll, C. (1998), Recovering surface temperature and emissivity from thermal infrared multispectral data. *Remote Sens. Environ.* 65:121–131.

Yamaguchi, Y., Kahle, A., Tsu, H., Kawakami, T., and Pniel, M. (1998), Overview of Advanced Spaceborne Thermal Emission Reflection Radiometer, (ASTER). *IEEE Trans. on Geo. Remote Sens.* 36:1062–1071.